Syndiotactic- and heterotactic-specific radical polymerization of *N*-*n*-propylmethacrylamide complexed with alkali metal ions

Tomohiro Hirano,[a]* Tadashi Segata,[a] Junpei Hashimoto,[a] Yohei Miwa,[b] Miyuki Oshimura[a] and Koichi Ute[a]

[a]Department of Chemical Science and Technology, Institute of Technology and Science, Tokushima University, 2-1 Minamijosanjima, Tokushima 770-8506, Japan

[b]Department of Chemistry and Biomolecular Science, Faculty of Engineering, Gifu University, Yanagido, Gifu 501-1193, Japan

*Corresponding author. E-mail: hirano@tokushima-u.ac.jp

†Electronic supplementary information (ESI) available: ^{13}C NMR spectra of the C=O group of NNPMAAm in the presence of $MNTf_2$, changes in the chemical shifts of ^{1}H NMR spectra of the vinylidene group of NNPMAAm in the presence of $LiNTf_2$, relationship between the radical concentration and time, additional ESR spectra and relationship between the ΔT_c and $\overline{n}_r$ values. See DOI: 10.1039/b000000x/.

ABSTRACT

We investigated the radical polymerization of *N*-*n*-propylmethacrylamide (NNPMAAm) in the presence of alkali metal bis(trifluoromethanesulfonyl)imides ($MNTf_2$), in particular $LiNTf_2$. The addition of $MNTf_2$ led to a significant improvement in the yield and molecular weight of the resulting poly(NNPMAAm)s. Furthermore, the solvent employed influenced stereospecificity in the presence of $LiNTf_2$. The stoichiometry of the NNPMAAm–Li^+ complex appeared to be critical to determining the stereospecificity in the NNPMAAm polymerization. The 1:1-complexed monomer in protic polar solvents provided syndiotactic-rich polymers, whereas the 2:1-complexed monomer in aprotic solvents gave heterotactic-rich polymers. Stereochemical analyses revealed that *m*-addition by an *r*-ended radical was the key step in the induction of heterotactic specificity in the aprotic solvents. Spectroscopic analyses suggested that the Li^+ cation played a dual role in the polymerization process, with Li^+ stabilizing the propagating radical species and also activating the incoming monomer. Kinetic studies with the aid of electron spin resonance spectroscopy revealed that the addition of $LiNTf_2$ caused a significant increase in the k_p value and a decrease in the k_t value. The stereoregularity of poly(NNPMAAm)s was found to influence the phase transition behavior of their aqueous solutions. In a series of syndiotactic-rich polymers, the phase-transition temperature decreased gradually with increase in *rr* triad content. Furthermore, heterotactic-rich poly(NNPMAAm) exhibited high hysteresis, which increased in magnitude with increasing *mr* triad content.

INTRODUCTION

Methacrylates have been one of the most extensively studied classes of vinyl monomers in terms of stereoregularity since the first reports on the triad tacticities of poly(methy lmethacrylate)s (PMMAs) were determined by ^{1}H nuclear magnetic resonance (NMR) in 1960.[1-3] Methacrylates can be polymerized by a variety of polymerization systems including radical, anionic, and coordination mechanisms. Stereoregularity is a function of monomer structure, initiator, solvent, and temperature. As a result, control of a wide range of stereoregularities, such as isotacticity, syndiotacticity, and heterotacticity, has been achieved.[4]

However, stereochemical studies on the polymerization of *N*-alkylmethacrylamides (Fig. 1), which are amide analogs of methacrylates, are scarce.[5-12] This is mainly because *N*-alkylmethacrylamides can be polymerized only *via* a radical mechanism owing to their acidic N-H protons, which do not allow vinyl polymerizations *via* anionic and coordination mechanisms. In the case of *N*-alkylacrylamides, the N-H protons can be protected for anionic polymerizations. Indeed, stereoregular poly(*N*-isopropylacrylamide)s [poly(NIPAAm)s] were prepared by anionic polymerization of protected monomers, followed by deprotection.[13, 14] However, this protection strategy is unsuitable for *N*-alkylmethacrylamides, because *N*,*N*-disubstituted methacrylamides, which correspond to protected *N*-alkylmethacrylamides, show nonpolymerizability *via* any reaction mechanism,[15-20] unless the *N*-substituents are small and highly strained ring structures, such as aziridine

and azetidine.[21-23] Consequently, development of stereospecific radical polymerization is desired for the production of stereoregular poly(*N*-alkylmethacrylamide)s.

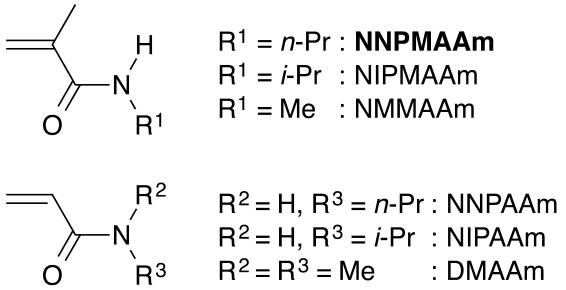

Fig. 1. Structures and abbreviations of methacrylamide and acrylamide derivatives described in this paper.

Although the stereoregularities of the poly(*N*-alkylmethacrylamide)s reported so far have been moderately syndiotactic,[5-12] a limited number of stereospecific radical polymerizations of *N*-alkylmethacrylamides have been reported in the last two decades.[24-28] For instance, poly(*N*-methylmethacrylamide) [poly(NMMAAm)] with *rr* triad = 95% was prepared in $(CF_3)_2CHOH$ at −78 °C.[24] Poly(*N*-isopropylmethacrylamide) [poly(NIPMAAm)] with *mm* triad = 67% was prepared in methanol at −20 °C in the presence of $Yb(OTf)_3$.[25, 26] Radical polymerization of bulky methacrylamides such as *N*-triphenylmethylmethacrylamide gave nearly 100% isotactic polymers.[28]

It is well known that Lewis acids, including alkali metal salts, accelerate the radical polymerization of (meth)acrylic monomers.[25-27, 29-41] Recently, we have also found that inclusion of alkali metal bis(trifluoromethanesulfonyl)imides ($MNTf_2$), such as $LiNTf_2$, in the radical polymerization of *N*,*N*-dimethylacrylamide (DMAAm) leads to

a significant increase in the yield and molecular weight of the resulting polymer.[42] NMR analysis of a mixture of DMAAm and $LiNTf_2$ suggests that DMAAm is activated by the coordination of Li^+ to its C=O group. Furthermore, electron spin resonance (ESR) spectroscopic analysis of the polymerization in the presence of $LiNTf_2$ suggests that the propagating radical is stabilized by Li^+, probably through a single-electron lithium bonding, which is a recently proposed theory.[43-47] Based on both of those effects, we have proposed a mechanism for this polymerization, where the propagation steps occur between a lithium ion-stabilized propagating radical and a lithium ion-activated incoming monomer. The activation effect of the incoming monomer is greater than the stabilizing effect of the Li^+ on the propagating radical, which leads to the polymerization-enhancing effect.

Furthermore, selecting the appropriate combination of solvent and alkali metal salt has successfully induced a wide range of stereospecificities, such as isotacticity, syndiotacticity, and heterotacticity, although stereocontrol of the polymerization of monosubstituted vinyl monomers has been recognized as difficult. The stereospecificities induced by $LiNTf_2$ in acetonitrile (CH_3CN) were correlated with complex structures formed through the coordinating interaction between the C=O group and Li^+; the 1:1 complex induced isotactic specificity, whereas the 2:1 complex induced heterotactic specificity. It is therefore assumed that this strategy, stereocontrol by complex structure, may be extended to other vinyl monomers.

Accordingly, we investigated the effect of alkali metal ions, in particular Li^+,

on the radical polymerization behavior of *N*-alkylmethacrylamides. Among the poly(*N*-alkylmethacrylamide)s, poly(NIPMAAm) and poly(*N*-*n*-propylmethacrylamide) [poly(NNPMAAm)] are known to exhibit phase transition in water at critical temperatures.[48-55] In this study, NNPMAAm was chosen as the monomer, instead of NIPMAAm, because poly(*N*-*n*-propylacrylamide) [poly(NNPAAm)], which is an acrylamide analog of poly(NNPMAAm), exhibits a large degree of hysteresis in phase transition behavior in aqueous solution when stereosequence in poly(NNPAAm) is regulated to be syndiotactic and isotactic.[56-58] It is therefore expected that the stereoregularity of poly(NNPMAAm)s affects the phase transition behavior of their aqueous solutions.

EXPERIMENTAL

Materials

NNPMAAm was prepared in a way similar to the synthesis of NNPAAm.[56] Dimethyl 2,2′-azobisisobutyrate (MAIB) (supplied by Otsuka Chemical Co., Ltd., Osaka, Japan) was recrystallized from methanol (CH_3OH). Toluene (Kanto Chemical Co., Inc., Tokyo, Japan) was purified by washing with sulfuric acid, water, and 5% aqueous NaOH, followed by fractional distillation. CH_3OH (Kanto Chemical Co., Inc.) was fractionally distilled. Ethanol (CH_3CH_2OH), $LiNTf_2$ (Tokyo Chemical Industry, Tokyo, Japan), tetrahydrofuran (THF), CH_3CN, *N*,*N*-dimethylformamide (DMF; high-performance liquid chromatography grade) (Kanto Chemical Co., Inc.), acetone, acetylacetone,

diethyl ether, deuterated dimethyl sulfoxide (DMSO-d_6), potassium bis(trifluoromethanesulfonyl)imide ($KNTf_2$) (Wako Pure Chemical Industries, Osaka, Japan), 2,2,2-trifluoroethanol (CF_3CH_2OH), 4-hydroxy-2,2,6,6-tetramethylpiperidine-1-oxyl (TEMPOL) (Sigma-Aldrich Japan, Tokyo, Japan), sodium bis(trifluoromethanesulfonyl)imide ($NaNTf_2$), and lithium bromide (LiBr, anhydride) (Kishida Chemical Co., Ltd, Osaka, Japan) were used as received.

Polymerization

In a typical polymerization procedure, NNPMAAm (1.27 g, 10.0 mmol), $LiNTf_2$ (1.44 g, 5.0 mmol), and MAIB (0.023 g, 10.0×10^{-2} mmol) were dissolved in CH_3CN to prepare 5 mL of solution. Four milliliters of the solution was transferred to a glass ampoule, which was degassed under vacuum and filled with nitrogen six times at −50 °C before the temperature was raised to the required polymerization temperature. Under reduced pressure, the mixture was irradiated at a distance of *ca*. 5 cm by a UV-LED lamp (LED-41UV375N100VF, λ = 375 nm, 410 mW, Optocode Co., Tokyo, Japan) to initiate polymerization. (The glass ampoule was placed at 40 °C or 60 °C when NNPMAAm was thermally polymerized.) After 24 h, the reaction mixture was dialyzed against CH_3OH/acetone (1:1 vol/vol) containing a small amount of acetylacetone (Spectra/Por 3, molecular mass cutoff 3.5 kDa, Spectrum Laboratories Inc., Shiga, Japan) until it was free from salts. The dialysate was evaporated to dryness under reduced pressure to give

a residue, which was dissolved in THF and poured into diethyl ether (400 mL). The precipitated polymer was collected by centrifugation, and dried *in vacuo*. The polymer yield was determined gravimetrically.

Size-exclusion chromatography (SEC) measurement

The molecular weights and molecular weight distributions of the polymers were determined by SEC; the chromatograph was calibrated with standard PMMA samples. SEC was performed on an HLC 8220 chromatograph (Tosoh Corp., Tokyo, Japan) equipped with TSKgel columns [SuperHM-M (6.5 mm inner diameter × 150 mm) and SuperHM-H (6.5 mm inner diameter × 150 mm)] (Tosoh Corp.). DMF containing 10 $mmol \cdot L^{-1}$ LiBr was used as an eluent at 40 °C and a flow rate of 0.35 $mL \cdot min^{-1}$. The initial polymer concentration was set at 1.0 $mg \cdot mL^{-1}$.

NMR measurements

^{1}H and ^{13}C NMR spectra were measured on EX-400, ECX-400, ECA-400, and ECA-500 spectrometers (JEOL Ltd., Tokyo, Japan). Triad tacticities were determined from ^{13}C NMR signals of the quaternary carbons measured in DMSO-d_6 at 100 °C.[24, 25] Fig. 2 shows the 100 MHz ^{13}C NMR spectra of the quaternary carbons of the syndiotactic- and heterotactic-rich poly(NNPMAAm)s obtained in this study.

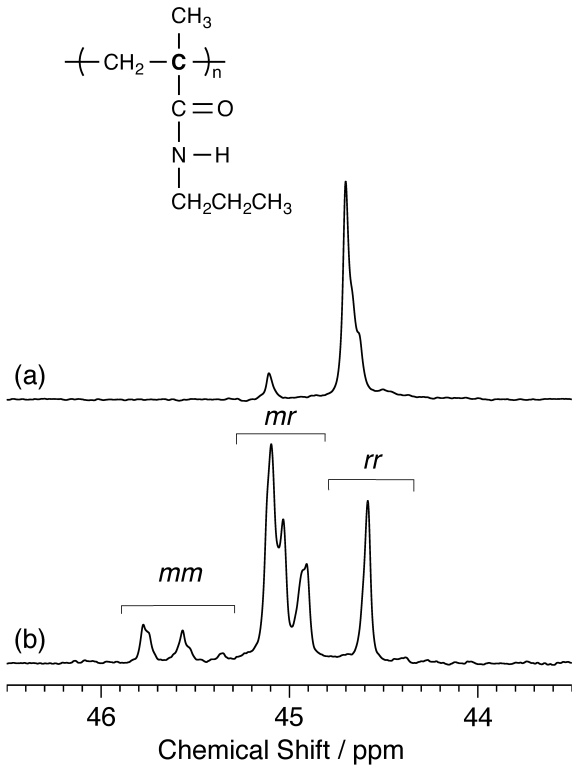

Fig. 2. 100 MHz ^{13}C NMR spectra of the quaternary carbons of (a) syndiotactic-rich and (b) heterotactic-rich poly(NNPMAAm)s.

ESR measurements

ESR samples were placed in 1-mm (outer diameter) quartz tubes and degassed by several freeze-pump-thaw cycles before being sealed under a nitrogen atmosphere. ESR spectra were recorded on an X-band (*ca*. 9 GHz) FA100 spectrometer (JEOL Ltd.) at 0 °C with 100 kHz field modulation. UV irradiation (350–370 nm) was carried out using an ultra-high-pressure mercury lamp (SX-UI501HQ; Ushio Ltd., Tokyo, Japan) with appropriate UVD-350 (AGC Techno Glass Co., Ltd., Shizuoka, Japan) and HAF-50S-30H (Sigma Koki, Co., Ltd., Saitama, Japan) glass filters.

Detection of propagating radical species

The following parameters were used to detect the propagating radical species: the modulation width, magnetic field width, sweep time, and time constant were set at 0.5 mT, 15 mT, 2 min, and 0.3 s, respectively. The number of scans was set at 1 ($LiNTf_2$) or 3 (none), depending on the radial concentrations. A microwave power of 5 mW was used for the measurements. The magnetic field and *g* tensor were calibrated with Mn^{2+}. The concentration of the propagating radical species was determined by the double integration of the ESR signal and a comparison of this result with that corresponding to the ESR spectrum of a known concentration of TEMPOL in CH_3CN.

Time-resolved ESR measurement

To measure the decrease in the TEMPOL radical concentration during the polymerization with an interval of several tens of seconds, the time-resolved measurement was performed using a package program with the following parameters: the modulation width, magnetic field width, sweep time, time constant, microwave power, and number of scans were set at 0.2 mT, 1 mT, 1 s, 0.001 s, 1 mW, and 1, respectively. Of the triplet signals of TEMPOL, the signal at the lowest magnetic field was monitored.

RESULTS AND DISCUSSION

Radical polymerization of NNPMAAm in several solvents at 0 °C in the presence or absence of $LiNTf_2$

Radical polymerizations of NNPMAAm were carried out in various solvents at 0 °C in the presence or absence of a 0.5 mole equivalent of $LiNTf_2$ relative to the NNPMAAm monomer (Table 1). The addition of $LiNTf_2$ increased significantly the polymer yield and number-average molecular weight (M_n), except for THF. Coordinating ability of THF to Li^+ would be responsible for suppressing the addition effect of $LiNTf_2$. These results correspond to those observed for the DMAAm polymerizations.[42]

<Table 1>

The stereoregularities of the poly(NNPMAAm)s were also affected by the addition of $LiNTf_2$. In addition, the solvent played an important role in determination of stereospecificity. For example, syndiotactic-rich polymer with *rr* triad = 71.0% was obtained in CH_3OH in the presence of $LiNTf_2$, although the *rr* triad decreased by 6.9% with the addition of $LiNTf_2$. The tendency of decreasing *rr* triad in the presence of $LiNTf_2$ was enhanced as the polarity of protic solvents decreased. On the other hand, the *mr* triad was increased by adding $LiNTf_2$ to the NNPMAAm polymerizations in aprotic solvents, regardless of the polarity. In particular, the heterotactic-rich polymer with *mr* triad = 64.4% was obtained in CH_3CN; the increase in the *mr* triad reached

40.3%.

The conditional probabilities for *m*-addition and *r*-addition in the propagating reaction, (*i.e.*, the so-called first-order Markovian-statistics parameters, such as $P_{r/m}$ and $P_{m/r}$) are also summarized in Table 1. For example, the parameter $P_{r/m}$ denotes the probability of an *m*-addition by an *r*-ended radical (Scheme 1). When the polymer propagation obeys Bernoullian statistics, $P_{r/m}$ will be equal to $P_{m/m}$ and $P_{m/r}$ will be equal to $P_{r/r}$. The equivalent relation, $P_{r/m} + P_{m/r} = 1$, is a useful measure for testing the extent to which the system obeys Bernoullian statistics; complete deviations from Bernoullian statistics result in a ($P_{r/m} + P_{m/r}$) value of either zero or two. The sums of $P_{r/m}$ and $P_{m/r}$ are listed in Table 1.

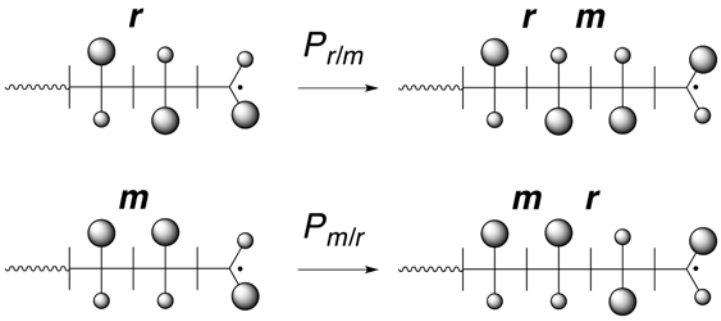

Scheme 1. Heterotactic propagations by the *r*-ended and *m*-ended radicals and the first-order Markovian-statistics parameters.

The values for the polymers obtained in the absence of $LiNTf_2$ were reasonably close to unity, regardless of the solvent used; the deviations were within 6.8%. These results demonstrate that the stereosequences in the poly(NNPMAAm)s radically prepared at 0 °C almost obey Bernoullian statistics. The value for the polymer obtained in CH_3OH

was also close to unity even though $LiNTf_2$ was added, whereas the values for the polymers obtained in protic, less polar solvents and aprotic solvents in the presence of $LiNTf_2$ significantly deviated from unity, and the deviation reached 37.4%. This is because the *mr* triad content, which can be attained in Bernoullian statistics, is at most 50%.[59]

Radical polymerization of NNPMAAm in CH_3OH or CH_3CN in the presence or absence of $LiNTf_2$

The polymer with the highest *rr* triad content was obtained in CH_3OH, whereas that with the highest *mr* triad content was obtained in CH_3CN. Therefore, the NNPMAAm polymerizations in CH_3OH and CH_3CN were investigated in more detail. Radical polymerizations of NNPMAAm were carried out in CH_3OH at a wide range of temperatures for 24 h in the absence of $LiNTf_2$ (Table 2; runs 13–17). Polymers were obtained in moderate yields, except for thermal polymerization at 60 °C. For example, the polymer was obtained at 31% yield when polymerized at 20 °C for 24 h. Polymer yield decreased as the polymerization temperature decreased, and polymerization scarcely proceeded at −40 °C under the given conditions, even though the polymerization time was extended up to 40 h (Table 2; run 17).

<Table 2>

Addition of $LiNTf_2$ increased polymer yield (Table 2; runs 18–24). As a result of an acceleration effect, the polymer was obtained at 8% yield even at −80°C, whereas reaction with NNPMAAm produced no polymers, at least it did not under the given conditions. One of the greatest advantages associated with being able to reduce the reaction temperature with the aid of $LiNTf_2$ is formation of polymers with higher stereoregularities. The *rr* triad content increased gradually with a decrease in the polymerization temperature, although the addition of $LiNTf_2$ decreased the *rr* triad content of the polymers obtained compared with those in the absence of $LiNTF_2$. The *rr* triad content reached 91.8% at −80 °C. Note that the stereosequences in the poly(NNPMAAm)s radically prepared in CH_3OH almost obey Bernoullian statistics, regardless of the temperature. The addition of $LiNTf_2$ also increased the M_n of the polymers obtained. Reducing the temperature enhanced the tendency. For example, around 2-fold increase was observed in M_n at 60 °C with the addition of LiNTf2, whereas the increase was nearly 6-fold at −20°C.

Radical polymerizations of NNPMAAm were also carried out in CH_3CN at a wide range of temperatures for 24 h in the absence of $LiNTf_2$ (Table 2; runs 25–28). Similar tendencies to those in CH_3OH were observed in the polymer yield, M_n, and stereoregularity. Polymer yield and M_n decreased as the polymerization temperature decreased, and polymerization scarcely proceeded at −20 °C under the given conditions. The *rr* triad content increased gradually as the temperature decreased.

The addition of $LiNTf_2$ exhibited a similar effect on the yield and M_n

compared with the NNPMAAm polymerizations in CH_3OH (Table 2; runs 29–31, 36, 37). On the other hand, heterotactic-rich polymers were obtained, regardless of the temperature. However, temperature dependence of the *mr* triad content was smaller than we expected. For example, polymers with *mr* triad contents of 62.0 and 62.9% were obtained at 60 and −20 °C, respectively. Instead of the *mr* triad, the *mm* and *rr* triad contents varied with the polymerization temperature; with a decrease in the temperature, the *mm* triad decreased gradually, whereas the *rr* triad increased gradually.

The ratio $P_{r/m}/P_{r/r}$ should correspond to the ratio of rate of *m*-addition and *r*-addition by *r*-ended radicals. Thus, $P_{r/m}$ / $P_{r/r}$ can be expressed as equation (1):

$$P_{r/m}/P_{r/r} = (k_{r/m}[P_r^{\bullet}][M])/(k_{r/r}[P_r^{\bullet}][M]) = k_{r/m}/k_{r/r} \quad (1)$$

where $[P_r^{\bullet}]$ and [M] are the concentrations of *r*-ended radical and monomer, and $k_{r/m}$ and $k_{r/r}$ are the rate constants of *m*-addition and *r*-addition by the *r*-ended radicals, respectively. Therefore, the ratio $P_{r/m}/P_{r/r}$ corresponds to the heterotactic selectivity of the *r*-ended radicals, because formation of a heterotactic sequence requires two opposite stereoregulations, *m*-addition by the *r*-ended radicals and *r*-addition by the *m*-ended radicals, to occur in an alternate manner. Similarly, $P_{m/r}/P_{m/m}$ corresponds to the heterotactic selectivity of the *m*-ended radicals.

Temperature dependences of the heterotactic selectivities of the *r*-ended and *m*-ended radicals in the NNPMAAm polymerizations in CH_3OH and CH_3CN in the

presence or absence of $LiNTf_2$ were examined. Fig. 3 shows Arrhenius plots of heterotactic selectivities of the *m*-ended and *r*-ended radicals. The addition of $LiNTf_2$ increased significantly only the heterotactic selectivity of the *r*-ended radicals in CH_3CN. This means that *m*-addition by *r*-ended radicals was identified as the key step for induction of heterotactic specificity in the present system. Furthermore, with an increase in 1/T, the heterotactic selectivity of the *m*-ended radicals increased gradually, whereas that of the *r*-ended radicals decreased slightly. Such opposite dependences of the heterotactic selectivity on the temperature are responsible for the unique temperature dependence of the triad tacticities of the polymers obtained in CH_3CN in the presence of $LiNTf_2$.

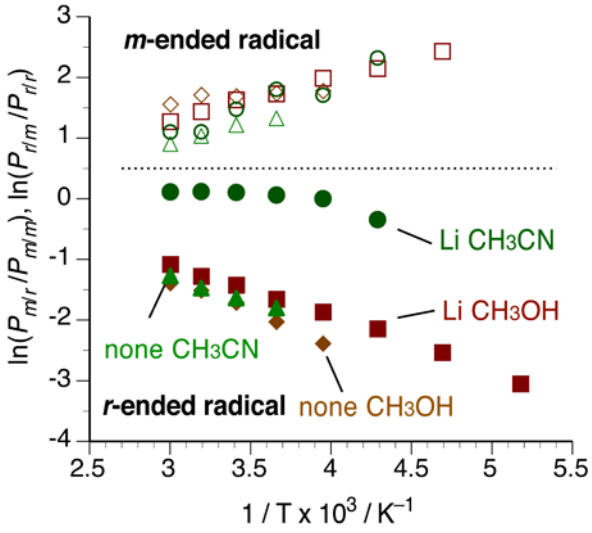

Fig. 3. Arrhenius plots of the heterotactic selectivities of the *r*-ended and *m*-ended radicals in the NNPMAAm polymerizations in CH_3OH and CH_3CN in the presence or absence of a 0.5 mole equivalent of $LiNTf_2$.

Effect of the $[LiNTf_2]_0/[NNPMAAm]_0$ ratio on the stereospecificity of the

polymerization in CH_3CN

To investigate the effect of the $[LiNTf_2]_0/[NNPMAAm]_0$ ratio on the induced heterotactic specificity, radical polymerizations of NNPMAAm were carried out in CH_3CN at 0 °C by changing the added amount of $LiNTf_2$ (Table 2; runs 32–35). Fig. 4 shows the changes in triad tacticities and polymer yields versus the $[LiNTf_2]_0/[NNPMAAm]_0$ ratio. The polymer yield significantly increased with the $[LiNTf_2]_0/[NNPMAAm]_0$ ratio but decreased over a ratio of 0.5. The *mr* triad content gradually increased, whereas the *rr* triad content gradually decreased, with the $[LiNTf_2]_0/[NNPMAAm]_0$ ratio, and the *mr* triad content became almost constant over a ratio of 0.5.

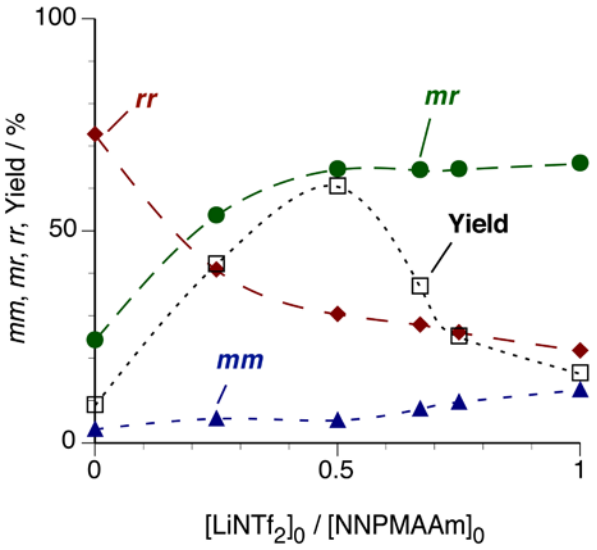

Fig. 4. Changes in triad tacticities and polymer yields versus the $[LiNTf_2]_0/[NNPMAAm]_0$ ratio in the NNPMAAm polymerization in CH_3CN at 0 °C.

Fig. 5 shows the relationship between the first-order Markovian parameters and the

$[LiNTf_2]_0/[NNPMAAm]_0$ ratio. The $P_{r/m}$ significantly increased with the $[LiNTf_2]_0/[NNPMAAm]_0$ ratio and the increasing tendency weakened over a ratio of 0.5. The $P_{m/r}$ slightly increased with the $[LiNTf_2]_0/[NNPMAAm]_0$ ratio and slightly decreased over a ratio of 0.5. These results suggest that the $[LiNTf_2]_0/[NNPMAAm]_0$ ratio = 0.5 is a critical point for the induction of heterotactic specificity in the NNPMAAm polymerization in CH_3CN.

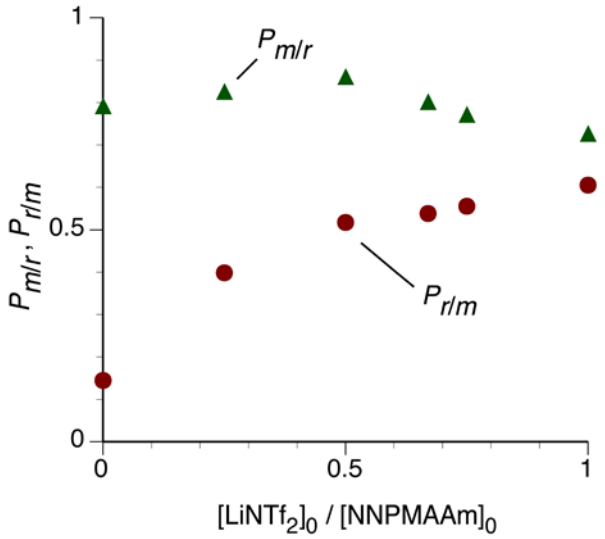

Fig. 5. Relationship between the first-order Markovian parameters and the $[LiNTf_2]_0/[NNPMAAm]_0$ ratio in the NNPMAAm polymerization in CH_3CN at 0 °C.

NMR study of complex formation between NNPMAAm and $LiNTf_2$

To develop a deeper understanding as to why the addition of $LiNTf_2$ dramatically enhanced the polymer yield and molecular weight, we investigated the nature of the interaction between the NNPMAAm monomer and Li^+ by examining changes in the chemical shifts of the NMR signals belonging to the methacryloyl group of

NNPMAAm upon mixing. The chemical shifts of the methacryloyl group are highly sensitive to the interaction between NNPMAAm and Li^+ as a result of the large changes in the intra- and intermolecular electron distributions following the coordination of Li^+. Fig. S1b (ESI†) shows the ^{13}C NMR spectrum of the C=O group in NNPMAAm following the addition of a 0.5 mole equivalent of $LiNTf_2$. The signal of the carbonyl carbon showed a large downfield shift of 1.04 ppm when the NNPMAAm was mixed with 50 mol% $LiNTf_2$. This result indicated that NNPMAAm formed a complex with Li^+ through a coordinating interaction between the C=O group of NNPMAAm and Li^+, as DMAAm and Li^+ do.[42]

The differences in the chemical shifts of the vinylidene group suggested that the complex formation enhanced the radical polymerizability of NNPMAAm (Table 3). The signals of both the H_1 and H_2 protons in the vinylidene group exhibited downfield shifts following the addition of $LiNTf_2$. The magnitude of the downfield shift was larger for the H_2 proton than the H_1 proton, and the difference in the chemical shifts between the H_1 and H_2 protons consequently increased from 0.360 to 0.384 ppm with the addition of $LiNTf_2$. There is a strong correlation between the difference in the chemical shifts of the vinylidene protons of methacrylates and the Q value of the monomer, in that the Q value increases as the chemical shift difference increases.[60] In addition, the signals of the C_α and C_β carbons exhibited upfield and downfield shifts, respectively, following the addition of $LiNTf_2$, resulting in a decrease of the chemical shift difference. Another correlation between the difference in the chemical shifts of the vinylidene

carbons of methacrylates and the 1/Q value of the monomer is that the 1/Q value decreases as the chemical shift difference decreases.[60]

<Table 3>

To investigate the stoichiometry of the NNPMAAm-Li^+ complex, ^1H NMR analyses were carried out on solutions with $[NNPMAAm]_0 + [LiNTf_2]_0 = 0.25\ mol \cdot L^{-1}$ in CD_3OD and CD_3CN at 0 °C. Fig. S2 (ESI†) shows changes in the chemical shift of the H_2 proton in the vinylidene group of NNPMAAm (*cf.* Table 3) resulting from variation of the initial proportion of NNPMAAm. The stoichiometry of the complex was evaluated by Job's method (Fig. 6) via equation (2):[61]

$$[NNPMAAm \cdot LiNTf_2] = \frac{\delta(H_2) - \delta(H_2)_f}{\delta(H_2)_c - \delta(H_2)_f} \times [NNPMAAm]_0 \quad (2)$$

where $\delta(H_2)$ and $\delta(H_2)_f$ are the chemical shifts of the sample mixture and NNPMAAm alone, respectively. The chemical shift of NNPMAAm varied with concentration as a result of self-association (ESI Fig. S2†). The chemical shift of NNPMAAm alone at the corresponding concentration was equated to $\delta(H_2)_f$. The chemical shift for the saturated mixture, $\delta(H_2)_c$, was calculated from the intercept of the quadratic fit to the data in Fig. S2 (ESI†), since the saturation value should be independent of NNPMAAm concentration.

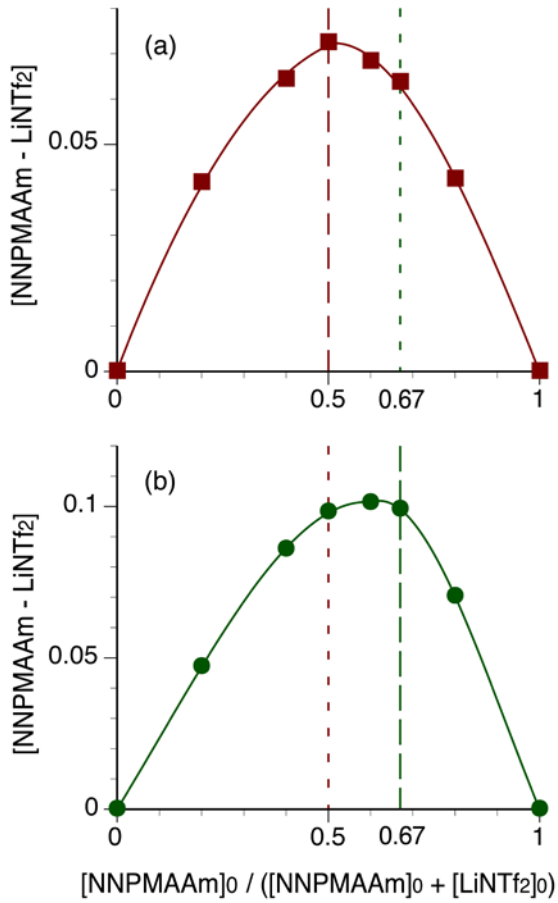

Fig. 6. Job's plots for the association of NNPMAAm with Li^+ in CD_3OD and CD_3CN at 0 °C.

A maximum was observed at an initial proportion of NNPMAAm = 0.5 in CD_3OD (Fig. 6a). This result indicates that NNPMAAm and Li^+ formed a 1:1 complex in methanol. However, a broad maximum was observed at an initial proportion of NNPMAAm = 0.6–0.67 in CD_3CN (Fig. 6b). This result suggests that NNPMAAm and Li^+ afford both 1:1 and 2:1 complexes, but the 2:1 complex is preferentially formed. It is therefore assumed that the stereospecificity of the NNPMAAm polymerization depends on the stoichiometry of the monomer–Li^+ complex; the 1:1 complex gave syndiotactic-rich polymers, whereas the 2:1 complex gave heterotactic-rich polymers. This dependence is

similar to that observed in the DMAAm polymerizations in CH_3CN in the presence of $LiNTf_2$.[42] It should be noted, however, that the 1:1 complex gave an isotactic-rich polymer in the DMAAm polymerizations. This is because the α-methyl group in NNPMAAm is responsible for the induction of syndiotactic specificity.

Proposed mechanism for the heterotactic specificity induced in CH_3CN in the presence of $LiNTf_2$

A heterotactic sequence can be formed by cyclopolymerization of divinyl monomers, where intra- and intermolecular additions occur alternately, and these two processes exhibit the opposite stereoselections, *m*- and *r*-addition. Kämmerer *et al*.[62] reported that heterotactic-rich PMMA (*mr* = 52%) was obtained by cyclopolymerization of 2,2'-methylenebis(4-methyl-2,1-phenylene)dimethacrylate, followed by hydrolysis and methylation. By a similar mechanism, heterotactic polymers were prepared by radical polymerization, in which 4-vinylpyridine formed a 2:1 inclusion complex with randomly methylated β-cyclodextrin.[63]

The Job's plots suggested that NNPMAAm and Li^+ preferentially form a 2:1 complex in CD_3CN. It is therefore assumed that this 2:1 complex behaves like a divinyl monomer. Thus, we propose the mechanism for the heterotactic specificity in the current system summarized in Scheme 2. At first, the pseudo-divinyl monomer approaches the propagating radical intermolecularly to reduce the electrostatic repulsion between the Li^+ binding to the monomeric unit at the chain end and the incoming

monomers. Subsequent pseudo-intramolecular propagation forms the *r* configuration at the second diad from the newly formed propagating chain end. The single bond near the *r*-ended propagating chain end is restricted by the coordinating interaction of the Li^+ with the amide groups at the penultimate and chain end monomeric units. Therefore, subsequent pseudo-intermolecular propagation forms the *m* configuration at the second diad from the newly formed propagating chain end. This *m*-ended radical is transformed to the *r*-ended radical by the subsequent pseudo-intramolecular propagation. As a result, *m*-addition by *r*-ended radicals and *r*-addition by *m*-ended radicals both take place in an alternating manner, leading to the formation of heterotactic stereosequences.

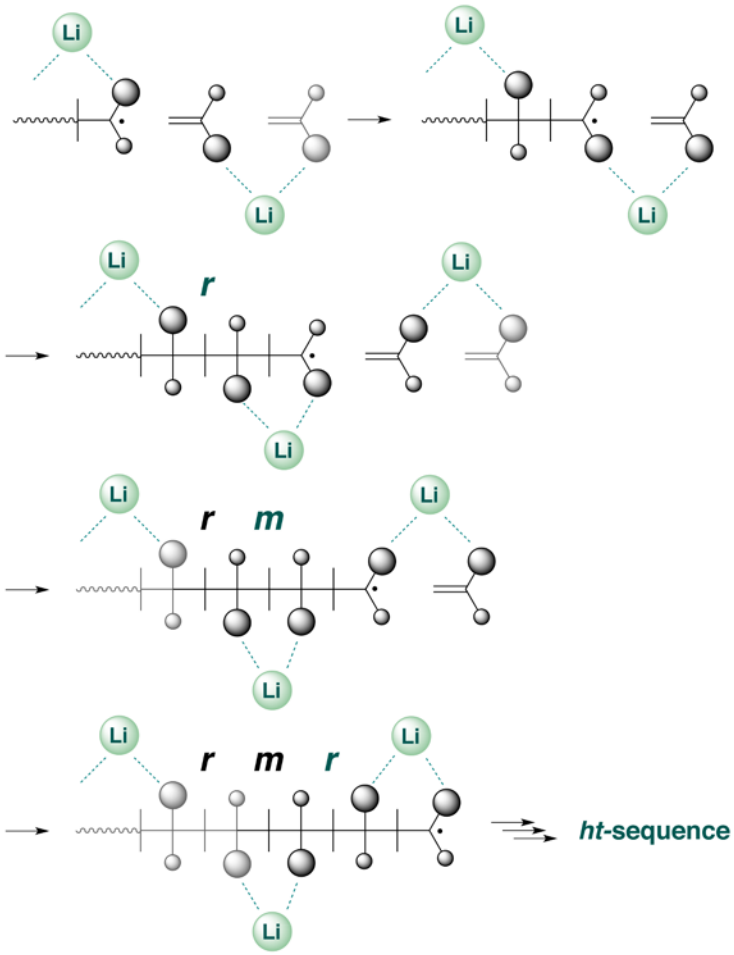

Scheme 2. Proposed mechanism for the heterotactic propagation by 2:1-complexed monomers.

ESR study of the NNPMAAm polymerization

ESR is a powerful tool for estimating the concentration of propagating radicals.[64, 65] However, reports on ESR spectra of the radical polymerizations of methacrylamides are limited.[11, 12, 66-69] Furthermore, almost all of the reports are concerned with radicals trapped in a variety of solid matrices.[66-69] This is probably because the radical concentration of the propagating radicals derived from methacrylamides is too low to be detected under practical conditions, owing to the cross-conjugation between the

C=C-C=O and O=C-N-H groups in methacrylamides.[16] It has been reported that addition of Li salts sufficiently increases radical concentration to an ESR-detectable level.[40, 42] For example, in the polymerization of DMAAm, ESR signals of the propagating radicals in solution were observed for the first time following addition of $LiNTf_2$.[42] Therefore, we conducted an ESR study of the NNPMAAm polymerization. Fig. 7 shows ESR spectra of the polymerization of NNPMAAm (2.0 $mol \cdot L^{-1}$) with MAIB (1.0×10^{-1} $mol \cdot L^{-1}$) at 0 °C in CH_3CN in the presence and absence of $LiNTf_2$ (1.0 $mol \cdot L^{-1}$). The 9-line spectra, characteristic of the polymerization of methacrylic monomers, were observed.[64, 65, 70] The addition of $LiNTf_2$ resulted in a significant increase in the concentration of the propagating radicals. During the ESR measurements, the observed spectra showed almost no change in intensities and shapes (ESI Fig. S3-5†), indicating that a stationary state with respect to the propagating radical was reached under the practical polymerization conditions. The stationary concentrations of the polymer radicals ($[P^{\bullet}]$) in the presence and absence of $LiNTf_2$ were determined to be 4.7×10^{-6} and 0.91×10^{-6} $mol \cdot L^{-1}$, respectively. This means that the radical concentration increases *ca.* five times following addition of $LiNTf_2$.

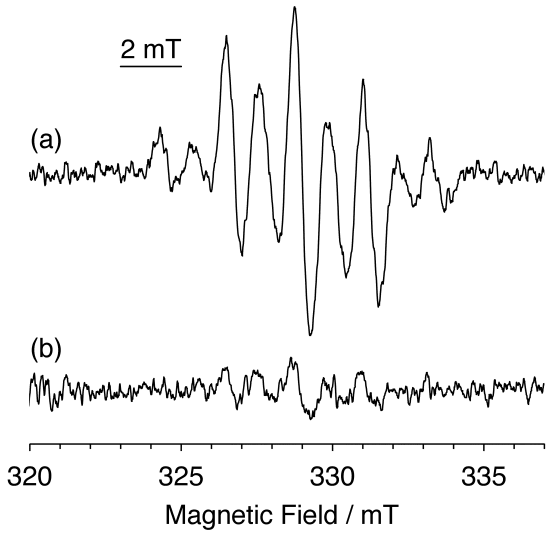

Fig. 7. ESR spectra of the NNPMAAm polymerization in CH_3CN at 0 °C in the (a) presence and (b) absence of $LiNTf_2$.

Fig. 8 shows time-conversion curves during the ESR measurements. The monomer conversions were determined by ^1H NMR spectra of the polymerization mixtures, which were obtained under the same conditions as the ESR measurements. The conversion increased linearly with time without any induction period in the early stage of polymerization, regardless of the presence or absence of $LiNTf_2$. The initial polymerization rates (R_p) in the presence and absence of $LiNTf_2$ were estimated to be 3.9×10^{-4} and 0.33×10^{-4} mol·L^{-1}·s^{-1}, respectively, from the time-conversion curves. The rate constants of propagation (k_p) in the presence and absence of $LiNTf_2$, therefore, were estimated to be 41 and 18 L·mol^{-1}·s^{-1}, respectively, according to equation (3):

$$R_p = k_p[P^{\bullet}][NNPMAAm] \quad (3)$$

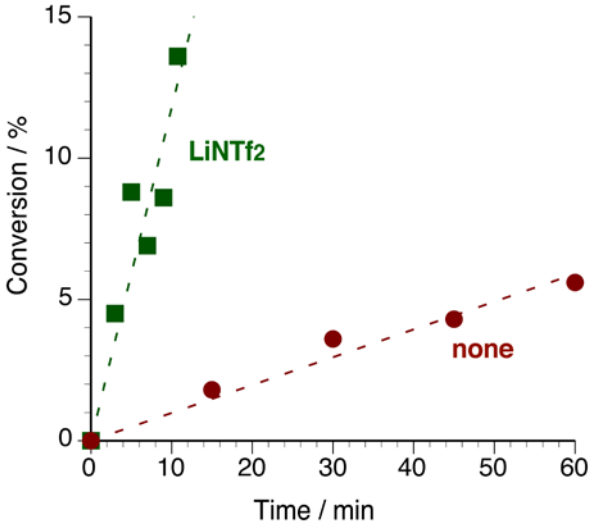

Fig. 8. Time-conversion curves for the polymerization of NNPMAAm with MAIB in the presence and absence of $LiNTf_2$.

The rate constant of termination (k_t) can be determined from the decay of the propagating polymer radicals formed in the polymerization. However, this method is unsuitable in the current system, because of the low concentration of the propagating radical in the absence of $LiNTf_2$. Therefore, to estimate the apparent k_t, the $k_d f$ values were determined using radical trapping method with TEMPOL under polymerization conditions,[71] where k_d and f denote rate constants of the MAIB decomposition and initiator efficiency, respectively. The reactions depicted in Scheme 3 proceed in the presence of TEMPOL in the polymerization. Some of the primary radicals derived from MAIB are deactivated by cage reactions. The others diffuse through the solvent cage, and react with NNPMAAm, followed by TEMPOL or with TEMPOL directly to yield coupling products. The $k_d f$ values, therefore, can be determined by monitoring the concentration of TEMPOL with the aid of ESR.

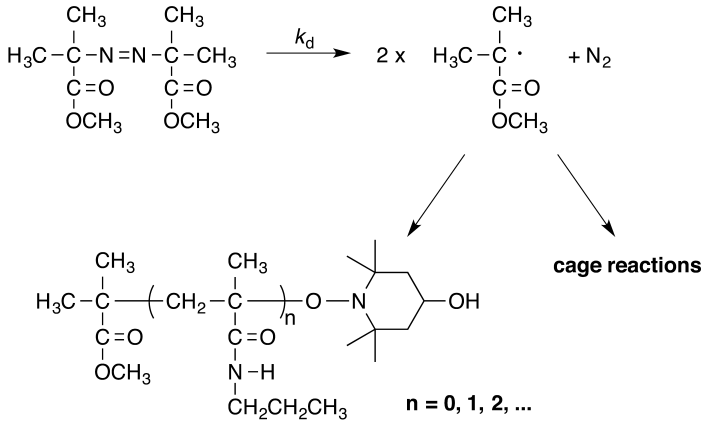

Scheme 3. Reactions of the primary radicals derived from MAIB in NNPMAAm polymerization in the presence of TEMPOL.

Fig. 9 shows the relationship between reaction time and TEMPOL concentration in CH_3CN at 0 °C in the presence and absence of $LiNTf_2$ (1.0 mol·L^{-1}), where the initial concentrations of NNPMAAm, MAIB, and TEMPOL were 2.0, 1.0 × 10^{-1}, and 3.4 × 10^{-3} mol·L^{-1}, respectively. The k_df values in the presence and absence of $LiNTf_2$ were estimated to be 4.5 × 10^{-5} and 6.4 × 10^{-5}·s^{-1}, respectively, from the slopes of the straight lines. Some Lewis acids are reported to accelerate decomposition of MAIB in thermal polymerizations.[35, 36, 72, 73] Nevertheless, the k_df value was decreased following addition of $LiNTf_2$. It is therefore assumed that the initiator efficiency is significantly reduced at 0 °C by adding $LiNTf_2$.

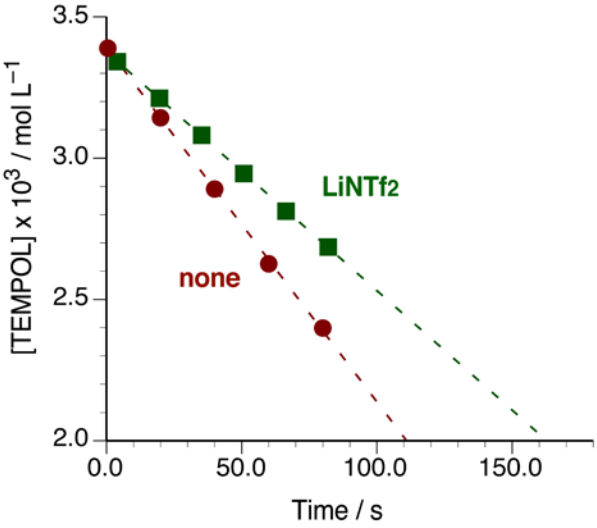

Fig. 9. Relationship between reaction time and concentration of TEMPOL during the polymerization of NNPMAAm with MAIB in CH_3CN at 0 °C.

Then the k_t values were calculated using equation (4):

$$2k_d f[\mathrm{MAIB}] = 2k_t[\mathrm{P}^\bullet]^2 \quad (4)$$

This is because bimolecular termination essentially occurs in radical polymerization, even if Lewis acids such as Li salts exist in the polymerization system.[35, 36] Note the use of the definition of the rate of termination (R_t) based on the IUPAC recommendation,[74, 75] instead of $R_t = k_t[\mathrm{P}^\bullet]^2$. The calculated k_t values in the presence and absence of $LiNTf_2$ were 2.0×10^5 and 77×10^5 $L \cdot mol^{-1} \cdot s^{-1}$, indicating that the addition of $LiNTf_2$ leads to an approximately 36-fold decrease in the rate constant of the terminating reaction.

Effect of the cation on radical polymerization behavior of NNPMAAm in CH_3CN

at 0 °C

To examine the extent to which the cation affects the yield, molecular weight, and stereoregularity of the polymer, $NaNTf_2$ and $KNTf_2$ were added to the NNPMAAm polymerization in CH_3CN at 0 °C instead of $LiNTf_2$. The addition of $NaNTf_2$ and $KNTf_2$ enhanced the polymer yields, molecular weights, and *mr* triad contents. However, their magnitudes decreased gradually in the order: $Li^+ > Na^+ > K^+$ (Fig. 10).

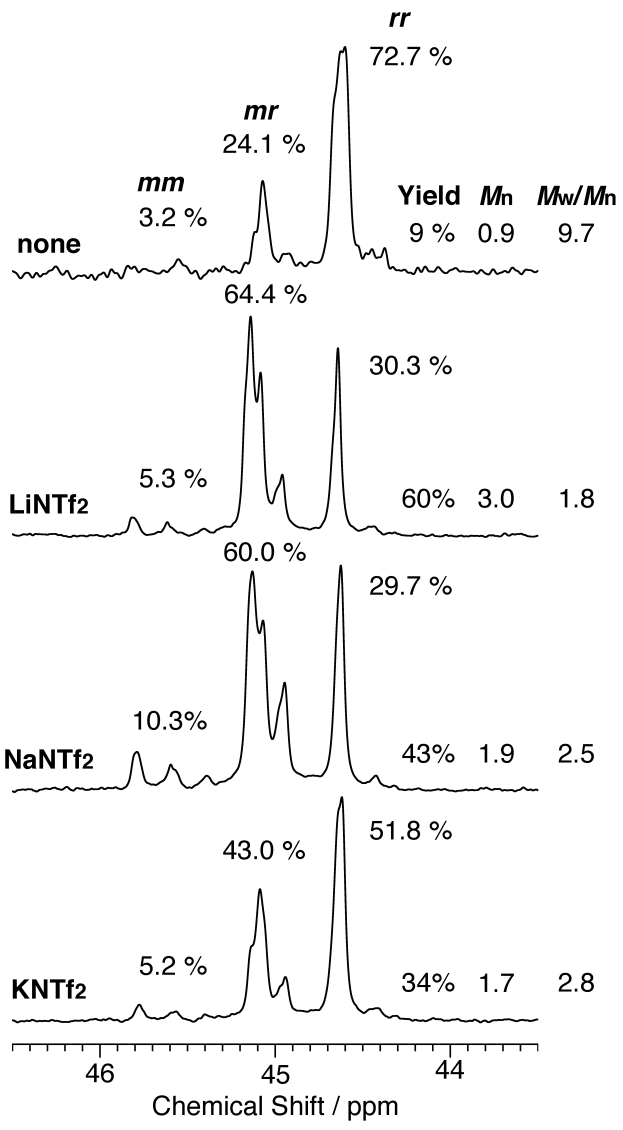

Fig. 10. 100 MHz ^{13}C NMR spectra of the quaternary carbons of poly(NNPMAAm)s prepared in CH_3CN at 0 °C in the presence or absence of $MNTf_2$.

The ^{13}C NMR signals of the C=O groups of NNPMAAm showed downfield shifts following addition of the alkali metal salts (ESI Fig. S1†). However, the magnitude of the downfield shift decreased gradually in the order: $Li^+ > Na^+ > K^+$. Furthermore, the difference in the chemical shifts between the vinylidene protons increased with the addition of $NaNTf_2$ and $KNTf_2$, as well as $LiNTf_2$ (Table 3). However, the magnitude decreased gradually in the order: $Li^+ > Na^+ > K^+$. These results suggest that the coordinating interaction between the NNPMAAm and the alkali metal cation decreased in the same order.

Effect of stereoregularity on the phase transition behavior of aqueous solution of poly(NNPMAAm)

An aqueous solution of poly(NNPMAAm) radically prepared in benzene at 73 °C exhibits phase transition at *ca.* 28 °C, although the NNPMAAm monomer is insoluble in water.[48, 54, 55] Therefore, we examined the effect of syndiotacticity on phase transition behavior. Fig. 11 shows the temperature dependences of the transmittances (500 nm) of aqueous solutions of syndiotactic-rich poly(NNPMAAm)s with *rr* triad contents of 63.3, 71.0, 80.4, and 91.8% (*cf.* runs 2, 4, 22, and 24). The phase-transition temperature in the heating process decreased gradually as the *rr* triad content increased (Fig. 11a). It should be noted that this tendency is the opposite to that of the aqueous poly(NIPMAAm)s, for which the phase-transition temperature of the poly(NIPMAAm)

with *rr* = 80% was higher than that of the poly(NIPMAAm) with *mm* = 67%.[25, 26] It is therefore assumed that higher syndiotacticity reduces the solubility of poly(NNPMAAm), probably because polymers with higher levels of stereoregularity are generally less soluble, as evidenced by several other polymers, including poly(*N*,*N*-dialkylacrylamide)s and poly(*N*-alkylacrylamide)s.[58, 76-78]

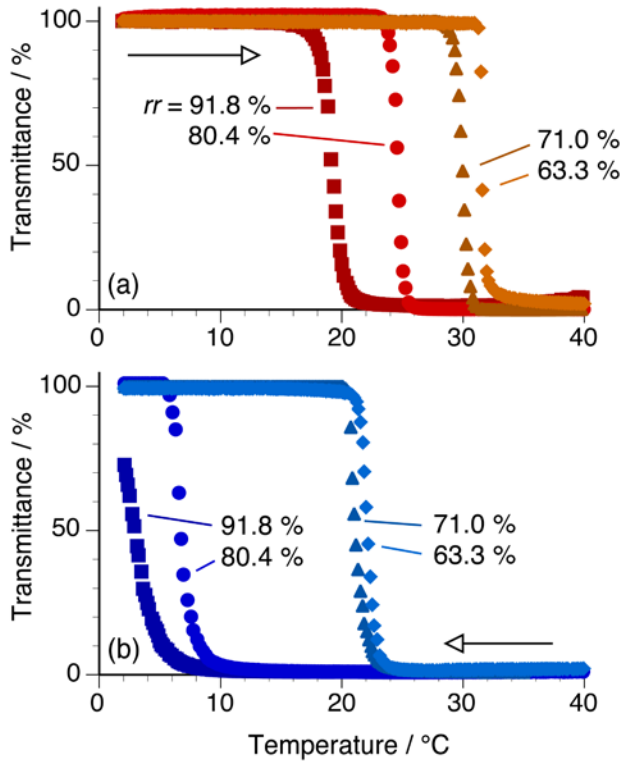

Fig. 11. Temperature dependence of the transmittance at 500 nm of the aqueous solution of syndiotactic-rich poly(NNPMAAm)s in (a) heating and (b) cooling processes. (0.1 w/v%, heating and cooling rates = 0.5 °C·min^{-1}).

The phase transitions in the cooling processes of the poly(NNPMAAm)s with *rr* triad content of 63.3 and 71.0% were observed at lower temperatures than those in the heating processes (Fig. 11b). The differences in T_c between the heating and cooling

processes (ΔT_cs) (8.8–9.5 °C) were larger than those observed for poly(NNPAAm)s with r = 60.4–65.5% under the corresponding measurement conditions (1.5–1.7 °C).[57] Taking into account that the heat of phase transition of aqueous poly(NNPMAAm) is larger than that of aqueous poly(NNPAAm),[48] the increased ΔT_c suggests that the introduction of methyl groups at the α positions of the monomeric units increased hydrophobicity, leading to an enhanced interaction between polymer chains in the dehydrated state.

Furthermore, the phase transition temperature of the poly(NNPMAAm)s with rr = 80.4 and 91.8% decreased drastically. Fig. S6 (ESI†) shows the relationship between the ΔT_c and the average length of the r diad ($\overline{n}_r$) in the syndiotactic-rich poly(NNPMAAm)s. The hysteresis was discontinuously enhanced at a certain $\overline{n}_r$ value; poly(NNPMAAm) with $\overline{n}_r$ over at least 9.69 exhibited high hysteresis over 16 °C. A similar tendency was observed for the aqueous poly(NNPAAm)s.[57] However, the critical $\overline{n}_r$ value (9.69) was quite large compared with that for poly(NNPAAm) (3.06). In previous papers,[57, 58] we have proposed that cooperative intramolecular hydrogen bonding among the amide groups of adjacent monomeric units in the syndiotactic stereosequences is responsible for induction of high hysteresis, because the formation of intramolecular hydrogen bonds makes dehydrated copolymers more hydrophobic (Scheme 4). The significant increase in the critical $\overline{n}_r$ value from 3.06 to 9.69 implies that the formation of the intramolecular hydrogen bonds is impeded in the dehydrated poly(NNPMAAm)s, because the introduction of methyl groups at the α position reduces

main-chain flexibility.[49, 79]

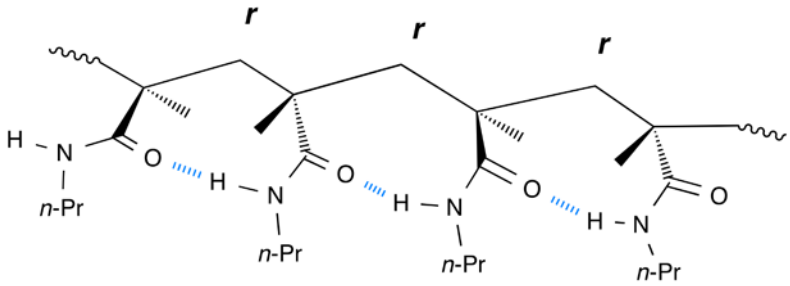

Scheme 4. Proposed intramolecular hydrogen bonding between amide groups in adjacent monomeric units in the syndiotactic stereosequence of the dehydrated poly(NNPMAAm).

Fig. 12 shows the temperature dependences of the transmittances of aqueous solutions of heterotactic-rich poly(NNPMAAm)s with *mr* triad contents of 64.4 and 57.0% (runs 8 and 37). The ΔT_c value increased from 8.9 to 14.8 °C with *mr* triad content increasing from 57.0 to 64.4%. This tendency is in complete contrast to that observed for aqueous poly(NIPAAm)s, for which the ΔT_c values of heterotactic poly(NIPAAm)s are smaller than those of syndiotactic and isotactic ones.[80] The mechanism for the enhanced hysteresis observed for heterotactic-rich poly(NNPMAAm)s is unclear. However, it is assumed that another type of intramolecular hydrogen bonding is formed to make the dehydrated heterotactic-rich poly(NNPMAAm)s hydrophobic; one possible explanation is cooperative intramolecular hydrogen bonding among the monomeric units skipping one monomeric unit (Scheme 5). Similar intramolecular hydrogen bonding has been calculated for the heterotactic trimer of NIPAAm.[81]

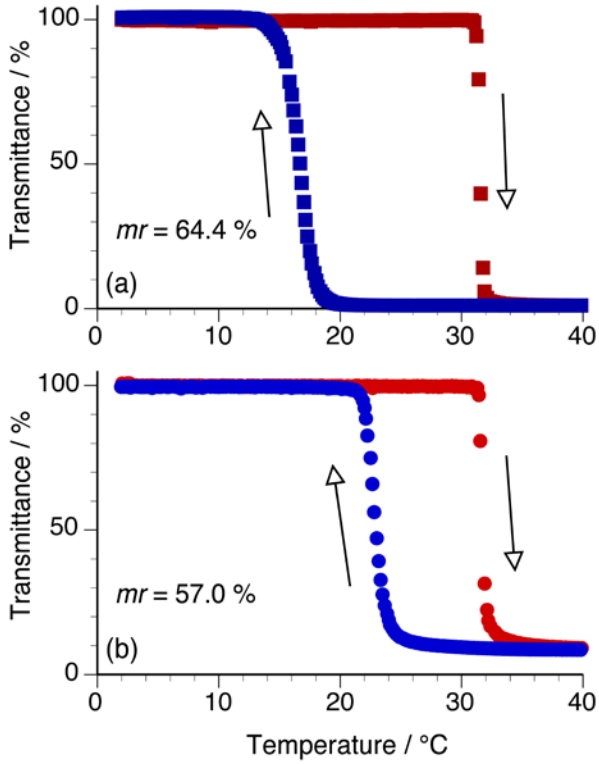

Fig. 12. Temperature dependence of the transmittance at 500 nm of the aqueous solution of heterotactic-rich poly(NNPMAAm)s with *mr* triad content of (a) 64.4% and (b) 57.0%. (0.1 w/v%, heating and cooling rates = 0.5 °C·min^{-1}).

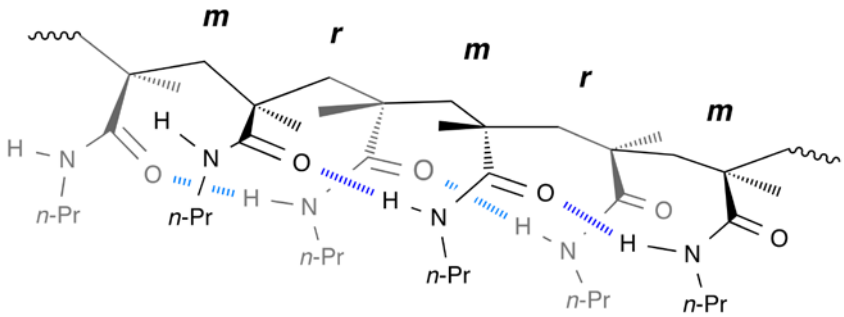

Scheme 5. Proposed intramolecular hydrogen bonding between amide groups in monomeric units skipping one monomeric unit in the heterotactic stereosequence of the dehydrated poly(NNPMAAm).

CONCLUSIONS

We investigated the effect of alkali metal bis(trifluoromethanesulfonyl)imides on the

radical polymerization of NNPMAAm. The addition of alkali metal salts led to a significant improvement in the yield and molecular weight of the resulting poly(NNPMAAm)s. Furthermore, the solvent influenced the stereospecificities in the presence of $LiNTf_2$; syndiotactic-rich polymers were obtained in protic polar solvents such as CH_3OH, whereas heterotactic-rich polymers were obtained in protic, less polar solvents such as CF_3CH_2OH and aprotic solvents such as CH_3CN. The stoichiometry of the NNPMAAm–Li^+ complex is critical to the stereospecificity in the NNPMAAm polymerization; the 1:1-complexed monomer provided syndiotactic-rich polymers, whereas the 2:1-complexed monomer gave heterotactic-rich polymers. Stereochemical analyses revealed that *m*-addition by *r*-ended radicals is the key step for the induction of heterotactic specificity in the present system.

Spectroscopic analyses suggested that the Li^+ cation plays a dual role in the polymerization process, with Li^+ stabilizing the propagating radical species and also activating the incoming monomer, as proposed for the DMAAm polymerization in the previous paper.[42] Kinetic studies with the aid of ESR spectroscopy revealed that the addition of $LiNTf_2$ caused a significant increase in the k_p value. A similar increase in the k_p value has been commonly observed for radical polymerizations of (meth)acrylic monomers in the presence of Lewis acids.[29-33, 35, 36, 39, 41]

The stereoregularity of poly(NNPMAAm)s was found to influence the phase transition behavior of their aqueous solutions. In a series of syndiotactic-rich polymers, the T_c decreased gradually with increasing *rr* triad content. This tendency is opposite to

that observed for poly(NIPMAAm).[25, 26] In addition, the poly(NNPMAAm)s with *rr* = 80.4 and 91.8% exhibited high hysteresis between the heating and cooling processes. The hysteresis in the phase-transition behavior can be explained by the intramolecular hydrogen bonding between contiguous NNPMAAm units in the syndiotactic sequence in the dehydrated state. However, the critical $\overline{n}_r$ value (9.69) was considerably larger than that for poly(NNPAAm) (3.06), suggesting that the formation of intramolecular hydrogen bonds was impeded in the less flexible poly(NNPMAAm)s in the dehydrated state, owing to the introduction of methyl groups at the α position. Furthermore, heterotactic-rich poly(NNPMAAm) exhibited high hysteresis, and the magnitude increased with increasing *mr* triad content. This result suggests that another type of intramolecular hydrogen bonding is formed to make the dehydrated heterotactic-rich poly(NNPMAAm)s hydrophobic, because heterotactic-rich poly(NIPAAm)s scarcely show hysteresis under the corresponding measurement conditions.[80]

ACKNOWLEDGMENT

This work was supported in part by KAKENHI [a Challenging Exploratory Research (22655035)].

REFERENCES

1. F. A. Bovey and G. V. D. Tiers, *J. Polym. Sci.*, 1960, 44, 173-182.
2. A. Nishioka, H. Watanabe, I. Yamaguchi and H. Shimizu, *J. Polym. Sci.*, 1960, 45, 232-234.
3. U. Johnsen and K. Tessmar, *Kolloid-Z*, 1960, 168, 160-161.
4. T. Hirano and T. Kitaura, in *Encyclopedia of Polymeric Nanomaterials*, eds. S. Kobayashi and K. Müllen, Springer Berlin Heidelberg, 2014, DOI: 10.1007/978-3-642-36199-9_216-1, ch. 216-1, pp. 1-25.

5. K. Hatada, T. Kitayama and K. Ute, *Polym. Bull.*, 1983, 9, 241-244.
6. C. Elvira and J. San Román, *Polymer*, 1997, 38, 4743-4750.
7. J. S. Román and A. Gallardo, *Polymer Engineering & Science*, 1996, 36, 1152-1162.
8. F. Sanda, M. Nakamura and T. Endo, *J. Polym. Sci., Part A: Polym. Chem.*, 1998, 36, 2681-2690.
9. B. Badey, P. Boullanger, A. Domard, P. Cros, T. Delair and C. Pichot, *Macromol. Chem. Phys.*, 1996, 197, 3711-3728.
10. A. Gallardo and J. S. Román, *Polymer*, 1993, 34, 394-400.
11. M. Seno, T. Fukui, T. Hirano and T. Sato, *J. Polym. Sci., Part A: Polym. Chem.*, 2000, 38, 4264-4271.
12. M. Seno, T. Yamada, H. Wang, T. Hirano and T. Sato, *J. Polym. Sci., Part A: Polym. Chem.*, 2005, 43, 2013-2020.
13. T. Kitayama, W. Shibuya and K.-i. Katsukawa, *Polym. J.*, 2002, 34, 405-409.
14. M. Ito and T. Ishizone, *J. Polym. Sci., Part A: Polym. Chem.*, 2006, 44, 4832-4845.
15. T. Otsu, M. Inoue, B. Yamada and T. Mori, *J. Polym. Sci.: Polym. Lett. Ed.*, 1975, 13, 505-510.
16. K. Yokota and J. Oda, *Kogyo Kagaku Zasshi*, 1970, 73, 224-228.
17. G. B. Butler and G. R. Myers, *J Macromol Sci: Part A - Chem*, 1971, 5, 135-166.
18. T. Kodaira and F. Aoyama, *J. Polym. Sci.: Polym. Chem. Ed.*, 1974, 12, 897-910.
19. T. Otsu, B. Yamada, T. Mori and M. Inoue, *J. Polym. Sci.: Polym. Lett. Ed.*, 1976, 14, 283-285.
20. J. Zábranský, M. Houska and J. Kálal, *Makromol. Chem.*, 1985, 186, 247-253.
21. N. Watanabe, Y. Sakakibara and N. Uciiino, *Kogyo Kagaku Zasshi*, 1969, 72, 1349-1352.
22. Y. Okamoto and H. Yuki, *J. Polym. Sci.: Polym. Chem. Ed.*, 1981, 19, 2647-2650.
23. T. Suzuki, J.-i. Kusakabe, K. Kitazawa, T. Nakagawa, S. Kawauchi and T. Ishizone, *Macromolecules*, 2010, 43, 107-116.
24. J. Zhang, W. Liu, T. Nakano and Y. Okamoto, *Polym. J.*, 2000, 32, 694-699.
25. S. Habaue, Y. Isobe and Y. Okamoto, *Tetrahedron*, 2002, 58, 8205-8209.
26. Y. Suito, Y. Isobe, S. Habaue and Y. Okamoto, *J. Polym. Sci., Part A: Polym. Chem.*, 2002, 40, 2496-2500.
27. Y. Isobe, Y. Suito, S. Habaue and Y. Okamoto, *J. Polym. Sci., Part A: Polym. Chem.*, 2003, 41, 1027-1033.
28. N. Hoshikawa, Y. Hotta and Y. Okamoto, *J. Am. Chem. Soc.*, 2003, 125, 12380-12381.
29. C. H. Bamford, A. D. Jenkins and R. Johnston, *Proc. Roy. Soc. London, Ser. A*, 1957, 241, 364-375.
30. V. F. Gromov, T. O. Osmanov, P. M. Khomikovskii and A. D. Abkin, *Eur. Polym. J.*, 1980, 16, 803-808.
31. D.-J. Liaw and K.-C. Chung, *Makromol. Chem.*, 1983, 184, 29-40.
32. V. A. Kabanov, *Makromol. Chem. Macromol. Symp.*, 1987, 10-11, 193-213.
33. J. Barton and E. Borsig, *Complexes in Free-Radical Polymerization*, Elsevier, Amsterdam, 1988.
34. M. A. Diab, A. Z. El-Sonbati, A. S. Hilali, H. M. Killa and M. M. Ghoneim, *Eur.*

Polym. J., 1990, 26, 1-3.
35. M. Seno, N. Matsumura, H. Nakamura and T. Sato, *J. Appl. Polym. Sci.*, 1997, 63, 1361-1368.
36. H. Nakamura, M. Seno and T. Sato, *J. Polym. Sci., Part A: Polym. Chem.*, 1997, 35, 153-162.
37. A. Matsumoto and S. Nakamura, *J. Appl. Polym. Sci.*, 1999, 74, 290-296.
38. Y. Isobe, D. Fujioka, S. Habaue and Y. Okamoto, *J. Am. Chem. Soc.*, 2001, 123, 7180-7181.
39. S. Pedrón, J. Guzmán and N. García, *Macromol. Chem. Phys.*, 2011, 212, 860-869.
40. L. Hermosilla, P. Calle, P. Tiemblo, N. García, L. Garrido and J. Guzmán, *Macromolecules*, 2013, 46, 5445-5454.
41. B. B. Noble, L. M. Smith and M. L. Coote, *Polym. Chem.*, 2014, 5, 4974-4983.
42. T. Hirano, T. Saito, Y. Kurano, Y. Miwa, M. Oshimura and K. Ute, *Polym. Chem.*, 2015, 6, 2054-2064.
43. Y. Li, D. Wu, Z.-R. Li, W. Chen and C.-C. Sun, *J. Chem. Phys.*, 2006, 125, 084317-084317.
44. L. Zhi-Feng, Z. Yu-Quan, L. Hui-Xue, Z. Yuan-Cheng and Y. Sheng, *J. Mol. Struct. (THEOCHEM)*, 2010, 958, 48-51.
45. T. Clark, *J. Chem. Soc., Chem. Commun.*, 1986, 1774-1776.
46. A. H. C. Horn and T. Clark, *J. Am. Chem. Soc.*, 2003, 125, 2809-2816.
47. T. Clark, *J. Am. Chem. Soc.*, 2006, 128, 11278-11285.
48. S. Ito, *Kobunshi Ronbunshu*, 1989, 46, 437-443.
49. S. Fujishige, K. Kubota and I. Ando, *J. Phys. Chem.*, 1989, 93, 3311-3313.
50. K. Kubota, K. Hamano, N. Kuwahara, S. Fujishige and I. Ando, *Polym J*, 1990, 22, 1051-1057.
51. E. I. Tiktopulo, V. N. Uversky, V. B. Lushchik, S. I. Klenin, V. E. Bychkova and O. B. Ptitsyn, *Macromolecules*, 1995, 28, 7519-7524.
52. M. Netopilík, M. Bohdanecký, V. Chytrý and K. Ulbrich, *Macromol. Rapid Commun.*, 1997, 18, 107-111.
53. Y. Maeda, T. Nakamura and I. Ikeda, *Macromolecules*, 2001, 34, 8246-8251.
54. M. Kano and E. Kokufuta, *Langmuir*, 2009, 25, 8649-8655.
55. M. Kokufuta, S. Sato and E. Kokufuta, *Colloid. Polym. Sci.*, 2012, 290, 1671-1681.
56. T. Hirano, K. Nakamura, T. Kamikubo, S. Ishii, K. Tani, T. Mori and T. Sato, *J. Polym. Sci., Part A: Polym. Chem.*, 2008, 46, 4575-4583.
57. T. Hirano, H. Yamamoto and K. Ute, *Polymer*, 2011, 52, 5277-5281.
58. T. Hirano, A. Ono, H. Yamamoto, T. Mori, Y. Maeda, M. Oshimura and K. Ute, *Polymer*, 2013, 54, 5601-5608.
59. K. Hatada, T. Kitayama and K. Ute, *Prog. Polym. Sci.*, 1988, 13, 189-276.
60. K. Hatada, T. Kitayama, T. Nishiura and W. Shibuya, *Curr. Org. Chem.*, 2002, 6, 121-153.
61. V. M. S. Gil and N. C. Oliveira, *J. Chem. Educ.*, 1990, 67, 473-478.
62. H. Guéniffey, H. Kämmerer and C. Pinazzi, *Makromol. Chem.*, 1973, 165, 73-81.
63. R. Saito, Y. Saito, H. Kamoshita and Y. Tokubuchi, *J. Polym. Sci., Part A: Polym. Chem.*, 2012, 50, 3444-3451.

64. B. Yamada, D. G. Westmoreland, S. Kobatake and O. Konosu, *Prog. Polym. Sci.*, 1999, 24, 565-630.
65. M. Kamachi, *J. Polym. Sci., Part A: Polym. Chem.*, 2002, 40, 269-285.
66. R. Bensasson, A. Prevot-Bernas, M. Bodard and R. Marx, *J. Chim. Phys. Phys.-Chim. Biol.*, 1963, 60, 950.
67. A. H. Reine, O. Hinojosa and J. C. Arthur, *J. Appl. Polym. Sci.*, 1973, 17, 3337-3343.
68. H. Tanaka, T. Sato and T. Otsu, *Makromol. Chem.*, 1980, 181, 2421-2431.
69. T. Sato, M. Oka, H. Tanaka and T. Ota, *Eur. Polym. J.*, 1987, 23, 475-480.
70. L. Hermosilla, P. Calle, C. Sieiro, N. García, P. Tiemblo and J. Guzmán, *Chem. Phys.*, 2007, 340, 237-244.
71. T. Sato, A. Takarada, H. Tanaka and T. Ota, *Makromol. Chem.*, 1991, 192, 2231-2241.
72. T. Otsu and B. Yamada, *J Macromol Sci: Part A - Chem*, 1969, 3, 187-196.
73. B. Yamada, H. Kamei and T. Otsu, *J. Polym. Sci.: Polym. Chem. Ed.*, 1980, 18, 1917-1922.
74. M. Buback, M. Egorov, R. G. Gilbert, V. Kaminsky, O. F. Olaj, G. T. Russell, P. Vana and G. Zifferer, *Macromol. Chem. Phys.*, 2002, 203, 2570-2582.
75. C. Barner-Kowollik, M. Buback, M. Egorov, T. Fukuda, A. Goto, O. F. Olaj, G. T. Russell, P. Vana, B. Yamada and P. B. Zetterlund, *Prog. Polym. Sci.*, 2005, 30, 605-643.
76. K. Butler, P. R. Thomas and G. J. Tyler, *J. Polym. Sci.*, 1960, 48, 357-366.
77. M. Kobayashi, S. Okuyama, T. Ishizone and S. Nakahama, *Macromolecules*, 1999, 32, 6466-6477.
78. B. Ray, Y. Okamoto, M. Kamigaito, M. Sawamoto, K.-i. Seno, S. Kanaoka and S. Aoshima, *Polym. J.*, 2005, 37, 234-237.
79. Y. Tang, Y. Ding and G. Zhang, *J. Phys. Chem. B*, 2008, 112, 8447-8451.
80. T. Hirano, T. Kamikubo, Y. Okumura, Y. Bando, R. Yamaoka, T. Mori and K. Ute, *J. Polym. Sci., Part A: Polym. Chem.*, 2009, 47, 2539-2550.
81. E. Autieri, E. Chiessi, A. Lonardi, G. Paradossi and M. Sega, *J. Phys. Chem. B*, 2011, 115, 5827-5839.

Table 1. Radical polymerization of NNPMAAm in various solvents at 0 °C for 24 h in the presence or absence of $LiNTf_2$[a]

Run	Solvent	$[LiNTf_2]_0$ /mol·L^{-1}	Yield /%	Tacticity[b] /%			$M_n \times 10^{-4}$ [c]	M_w/M_n [c]	$P_{m/r}$[d]	$P_{r/m}$[e]	$P_{m/r} + P_{r/m}$
				mm	*mr*	*rr*					
1	CH_3OH	0.0	17	1.8	20.3	77.9	0.7	7.0	0.849	0.115	0.964
2	(ε = 32.7)	1.0	44	2.4	26.6	71.0	2.8	3.5	0.847	0.158	1.005
3	CH_3CH_2OH	0.0	11	1.0	22.3	76.7	0.9	11.0	0.918	0.127	1.045
4	(ε = 24.6)	1.0	19	2.9	33.8	63.3	2.8	4.4	0.854	0.211	1.065
5	CF_3CH_2OH	0.0	4	1.6	25.8	72.6	0.9	8.1	0.890	0.151	1.041
6	(ε = 2.03)	1.0	21	6.4	54.0	39.6	4.3	3.6	0.808	0.405	1.213
7	CH_3CN	0.0	9	3.2	24.1	72.7	0.9	9.7	0.790	0.142	0.932
8	(ε = 37.5)	1.0	60	5.3	64.4	30.3	3.0	1.8	0.859	0.515	1.374
9	THF	0.0	3	2.3	25.4	72.3	1.2	7.2	0.847	0.149	0.996
10	(ε = 7.58)	1.0	5	4.4	56.0	39.6	2.1	7.1	0.864	0.414	1.278
11[f]	Toluene	0.0	3	4.2	28.7	67.1	1.0	11.6	0.774	0.176	0.950
12[f]	(ε = 2.38)	1.0	31	15.1	56.7	28.2	13.9	3.2	0.652	0.501	1.153

[a]$[NNPMAAm]_0$ = 2.0 mol·L^{-1}, $[MAIB]_0 = 2.0 \times 10^{-2}$ mol·L^{-1}. The values in parentheses denote the dielectric constants (ε) of the solvents.
[b]Determined from ^{13}C NMR signals of the quaternary carbons in the main chain.
[c]Determined by SEC.
[d]$P_{m/r} = (mr/2)/(mm + mr/2)$.
[e]$P_{r/m} = (mr/2)/(rr + mr/2)$.
[f]For 4 h.

Table 2. Radical polymerization of NNPMAAm in CH_3OH or CH_3CN for 24 h in the presence or absence of $LiNTf_2$[a]

Run	Solvent	$[LiNTf_2]_0$ /mol·L^{-1}	Temp. / °C	Yield /%	Tacticity[b] /%			$M_n \times 10^{-4}$ [c]	M_w/M_n [c]	$P_{m/r}$ [d]	$P_{r/m}$ [e]	$P_{m/r} + P_{r/m}$
					mm	*mr*	*rr*					
13[f]	CH_3OH	0.0	60	81	3.4	31.9	64.7	2.7	1.9	0.824	0.198	1.022
14[f]	CH_3OH	0.0	40	24	2.7	29.6	67.7	11.2	2.2	0.846	0.179	1.025
15	CH_3OH	0.0	20	31	2.4	25.7	71.9	1.0	6.5	0.843	0.152	0.995
16	CH_3OH	0.0	-20	6	1.3	15.2	83.5	0.5	6.4	0.854	0.083	0.937
17[g]	CH_3OH	0.0	-40	~0	-	-	-	-	-	-	-	-
18[f,h]	CH_3OH	1.0	60	33	5.4	37.8	56.8	4.8	2.1	0.778	0.250	1.028
19[f,h]	CH_3OH	1.0	40	7	4.1	33.9	62.0	14.2	1.8	0.805	0.215	1.020
20	CH_3OH	1.0	20	24	3.1	31.1	65.8	1.9	1.9	0.834	0.191	1.025
21	CH_3OH	1.0	-20	9	1.6	22.9	75.5	2.9	2.3	0.877	0.132	1.009
22	CH_3OH	1.0	-40	12	1.1	18.5	80.4	3.0	2.2	0.894	0.103	0.997
23	CH_3OH	1.0	-60	8	0.6	13.4	86.0	2.3	6.3	0.918	0.072	0.990
24	CH_3OH	1.0	-80	8	0.1	8.1	91.8	3.3	1.7	0.976	0.042	1.018
25[f]	CH_3CN	0.0	60	88	6.8	33.6	59.6	1.8	2.1	0.712	0.220	0.932
26[f]	CH_3CN	0.0	40	29	5.3	29.9	64.8	8.2	2.2	0.738	0.187	0.925
27	CH_3CN	0.0	20	21	4.0	27.0	69.0	0.7	6.8	0.771	0.164	0.935
28	CN_3CN	0.0	-20	~0	-	-	-	-	-	-	-	-
29[f,h]	CH_3CN	1.0	60	81	10.3	62.0	27.7	5.2	2.2	0.751	0.528	1.279
30[f,h]	CH_3CN	1.0	40	19	10.3	62.1	27.6	14.6	3.0	0.751	0.529	1.280
31	CH_3CN	1.0	20	42	7.3	63.9	28.8	2.3	2.0	0.814	0.526	1.340
32	CH_3CN	0.5	0	42	5.7	53.5	40.8	2.3	6.9	0.824	0.396	1.220
33	CH_3CN	1.34	0	37	8.0	64.2	27.8	2.2	2.6	0.800	0.536	1.336
34	CH_3CN	1.5	0	25	9.6	64.4	26.0	3.0	2.8	0.770	0.553	1.323
35	CH_3CN	2.0	0	16	12.5	65.8	21.7	6.1	3.0	0.725	0.603	1.328
36	CH_3CN	1.0	-20	19	5.7	62.9	31.4	1.8	4.2	0.847	0.500	1.347
37	CN_3CN	1.0	-40	33	2.8	57.0	40.2	2.9	1.9	0.911	0.415	1.326

[a] $[NNPMAAm]_0 = 2.0$ mol·L^{-1}, $[MAIB]_0 = 2.0 \times 10^{-2}$ mol·L^{-1}.
[b] Determined from ^{13}C NMR signals of the quaternary carbons in the main chain.
[c] Determined by SEC.
[d] $P_{m/r} = (mr/2)/(mm + mr/2)$.
[e] $P_{r/m} = (mr/2)/(rr + mr/2)$.
[f] Thermally polymerized without UV-LED irradiation.
[g] For 40 h.
[h] For 4 h.

Table 3. ^{1}H and ^{13}C NMR chemical shifts for the vinylidene groups of NNPMAAm[a]

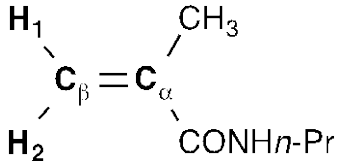

	δ_{H1}	δ_{H2}	$\lvert\delta_{H1} - \delta_{H1}\rvert$	$\delta_{C\alpha}$	$\delta_{C\beta}$	$\lvert\delta_{C\alpha} - \delta_{C\beta}\rvert$
none	5.305	5.665	0.360	141.42	119.42	22.00
$LiNTf_2$	5.388	5.772	0.384	140.08	121.69	18.39
$NNTf_2$	5.342	5.716	0.374	140.76	120.53	20.23
$KNTf_2$	5.323	5.696	0.373	141.04	120.06	20.98

[a]$[NNPMAAm]_0$ = 2.0 mol·L^{-1}, $[MNTf_2]_0$ = 0.0 or 1.0 mol·L^{-1}, in CD_3CN at 0 °C.